

# Analysis of the Principle and Applications for Surface Plasmon Polariton

Yuhan Liang

School of physics, Changchun University of Science and technology, Changchun, China

2020000288@mails.cust.edu.cn

**Abstract.** The integrated optics technology based on Surface Plasmon Polaritons (SPPs) is gradually emerging as a breakthrough for optical devices, owing to its high field localization and strong energy density. Currently, SPP-based technologies, such as optical modulators and wavelength filters, have demonstrated significant application value. However, the research on SPPs is predominantly focused on the visible and near-infrared bands due to difficulties in wavevector matching for excitation, insufficient theoretical investigations of SPPs, and limitations of micro-nanofabrication techniques. Consequently, research on SPPs in information transmission bands like the far-infrared is still scarce. Therefore, this paper starts from the electromagnetic theory fundamentals of SPPs and explores their redshift characteristics and excitation mechanisms. Subsequently, it summarizes research and modulation techniques in the infrared band, comparing and analyzing the advantages and limitations of optical devices based on the principles of SPPs. Finally, it presents some limitations of current SPP research and the development prospects of far-infrared devices.

**Keywords:** Surface plasmon polariton, optical modulator, infrared device.

## 1. Introduction

With the development of the data era, the limitations of traditional electronic devices are becoming more and more prominent, and the information technology of high transmission speed and large information capacity carrier is urgently needed. People focus on optical information transmission technology. Excitation of surface plasmon polaritons (SPPs), because of its high light field localization and extremely low deep subwavelength characteristic range, can break through the Abbe diffraction limit and further expand under the age of Moore's law [1]. The research process of SPPs can be traced back to Wood's first discovery of abnormal color brightness distribution in diffraction spectrum of metal gratings in 1902 [2]. This is not explained by grating theory, which also became the beginning of the study of SPPs phenomenon later. Later, in the mid-20th century, Rayleigh and Fano studied Wood's anomaly and put forward their own views and systematic explanations [3]. However, they did not link this phenomenon to the study of SPP [3]. It was not until the subsequent development of computer and the gradual refinement of the theory of plasma vibration and optical coupling that in 1974 Cunningham's team systematically calculated the surf-Plasmon dispersion curve by using a local approximation of the dielectric constant. In addition, the concept of Surface-plasmon-polaritons was introduced for the first time [4].

SPPs have a wide range of applications, mostly centered around their extremely small feature size and strong optical field density characteristics. Research on SPPs emerged in the late 20th century, and as early as 1983, there were already studies utilizing SPPs to determine the interaction between antibodies and antigens [5]. Subsequently, SPPs have been employed in various biological fields, such as high-sensitivity biosensing and molecular detection, taking advantage of their high sensing sensitivity [5]. In addition, SPPs have been used in areas like cancer treatment and pathogen detection, leveraging their strong near-field effects [5]. Apart from the biological domain, SPPs have found applications in fields such as laser optics, Raman spectroscopy, nonlinear optics, and integrated optics [1-6].

Currently, conventional metallic excitation materials for Surface Plasmon Polaritons (SPPs) are typically applied in the visible or near-infrared wavelength ranges, with aluminum being the sole

option in the ultraviolet region. However, research on SPP excitation in the mid to far-infrared regions is scarce. Therefore, this paper aims to explore the potential and principles of SPP excitation in the infrared wavelength range. Starting from the Maxwell's field equations of SPPs, it provides readers with a fundamental understanding of the electromagnetic and quantum concepts underlying SPP coupling modes. The redshift characteristic commonly observed in SPPs, as well as the challenging issue of wavevector matching known as the phase matching problem, are then introduced. Subsequently, the promising optical material graphene is discussed, highlighting its exceptional tunability and the limitless possibilities it offers for SPP infrared excitation structures. Finally, the paper summarizes practical applications of SPPs, emphasizing the advantages of SPP modulators through comparative analysis. Additionally, it presents some modulators and filters that have been investigated in the infrared domain.

## 2. Electromagnetic Theory of Surface plasmons

SPPs are coupled modes that arise from the interaction between an external electromagnetic field and surface plasmons in a material, propagating along the surface with exponential decay in the vertical direction [1]. They primarily originate from metals or materials with certain metallic properties and describe the collective motion of surface electrons [1]. By exciting different topological properties and boundary conditions of the material, SPPs can be categorized into two types: propagating modes, known as surface plasmon polaritons (SPPs), which are excited at the metal-dielectric interface, and localized modes, known as localized surface plasmon polaritons (LSPPs), which are excited on the surface of metal nanoparticles [6]. Electromagnetic excitation is the simplest form of SPPs [6]. One can consider a single-mode SPPs excitation model in a metal-dielectric interface, as shown in Fig. 1. For a newly formed electromagnetic wave coupling mode, the distribution of the electric field can be solved using Maxwell's electromagnetic theory.

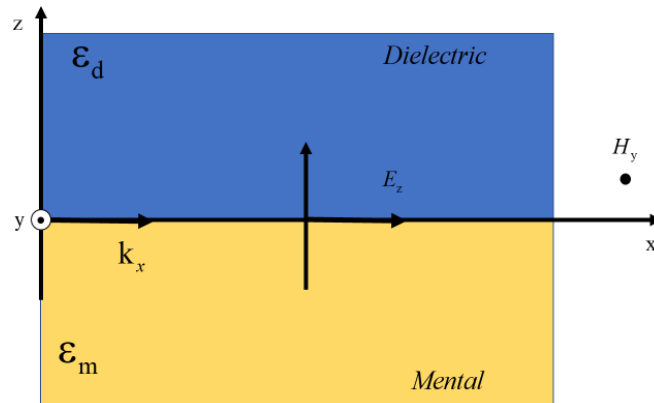


**Figure 1.** Schematic diagram of SPPs excitation

SPPs are excited at a single interface, where the z-axis positive half-space represents the dielectric region (typically air with a dielectric constant  $\epsilon_d$ ), and the z-axis negative half-space represents the quasi-metallic region (with a dielectric constant  $\epsilon_m$ , where the real part satisfies  $Re\{\epsilon_d\} < 0$ ). For computational convenience, one defines a TM wave, where the magnetic vector is perpendicular to the incident plane and oriented along the y-direction, while the wave vector in the x-direction is denoted as  $k_x$ . Maxwell equation solutions are

$$H_d = (0, A_d, 0) e^{-k_d z} e^{i(k_x x - \omega t)} \quad (1)$$

$$E_d = -A_d \left( \frac{ck_d}{i\epsilon_1 \omega}, 0, \frac{ck_x}{\epsilon_1 \omega} \right) e^{-k_d z} e^{i(k_x x - \omega t)} \quad (2)$$

In the region  $z > 0$ , and

$$H_m = (0, A_m, 0) e^{+k_m z} e^{i(k_x x - \omega t)} \quad (3)$$

$$E_m = -A_m \left( -\frac{ck_m}{i\varepsilon_m\omega}, 0, \frac{ck_x}{\varepsilon_m\omega} \right) e^{+k_m z} e^{i(k_x x - \omega t)} \quad (4)$$

In the region  $z < 0$ , where  $c$  and  $\omega$  are the speed of light and the circular frequency of incident light respectively,  $A_d$  and  $A_m$  are constants,

$$k_d = \sqrt{k_x^2 - \varepsilon_d \omega^2 / c^2}, k_m = \sqrt{k_x^2 - \varepsilon_m \omega^2 / c^2} \quad (5)$$

Are introduced variables, and the physical meaning is the wave vector component in the two media [1, 6]. From the solution of equations, it can be seen that the propagation direction of the electric vector in the x-direction is inconsistent in the two media, and the y-direction has the propagation characteristics of evanescent waves. According to the boundary conditions, one can also conclude that the real parts of the dielectric constants of the two materials satisfy the equation  $\varepsilon_d \varepsilon_m < 0$ . This is why noble metals are commonly used as materials for SPPs excitation. Studying a new optical coupling mode can provide insights into its electric field distribution characteristics and transmission properties through the dispersion relation. By rearranging the equation obtained from the relationship between wave vector and dielectric constant after squaring it, one obtains

$$k_{spp}(\omega) = \frac{\omega}{c} \sqrt{\varepsilon_d \varepsilon_m / (\varepsilon_d + \varepsilon_m)} \quad (6)$$

Which represents the SPP dispersion relation, where  $k_{spp}$  denotes the coupling wave vector of SPP [6]. The electric field distribution of SPPs exhibits nanoscale localization, being confined to micrometer-level in the propagation direction and decaying within sub-wavelength range in the perpendicular direction [7].

When the topology of the metal-medium interface is no longer an infinite plane, but a metal sphere particle with a certain radius, and the nanometer size is much smaller than the excitation wavelength, the propagation of SPPs is limited, resulting in the localized property, LSPP [6]. Therefore, it can be considered that LSPPs are solutions of the Maxwell's equations under a new electromagnetic boundary condition. LSPPs generally occur within the gaps of nano-particles or various topological structures, constrained by the geometric structures smaller than the propagation range ( $\delta_{spp}$ ). The surface plasmons in the material will resonate with incident light of specific wavelengths, which is why LSPPs are also referred to as Localized Surface Plasmon Resonance (LSPR). The theoretical treatment of LSPPs involves introducing a certain level of quantum theory correction based on the size of the structural features [8]. When the feature size is larger than 10nm, the classical Maxwell's electromagnetic theory can serve as a good approximation [8]. However, when the size is smaller than 10nm, additional considerations need to be taken into account, such as quantum confinement effects and the influence of quantum tunneling on the electric field [8]. Due to the specific boundary conditions imposed on LSPPs, they do not possess the characteristic parameters typically associated with propagating SPPs. Therefore, the physical properties of LSPPs are usually characterized through material interactions such as scattering, absorption, and attenuation [8]. Depending on the optical decay properties in different wavelength ranges, LSPPs can be applied in various fields.

### 3. Redshift of Surface Plasmons

Efficient SPPs-coupling materials have been discovered in the visible to near-infrared wavelength range [7]. Most commonly used materials include noble metals such as gold (Au), silver (Ag), palladium (Pd), and platinum (Pt), as well as some common alkali metals and conductor metals like copper and aluminum [7]. However, due to certain chemical or physical properties of each metal, there are drawbacks such as unstable excitation and difficult preservation. Currently, two-dimensional nanomaterials, such as graphene and black phosphorus, are considered as ideal excitation carriers for SPPs due to their high optical properties and tunable chemical structures, among other advantages [9]. Localized Surface Plasmon Polaritons exhibit sensitivity to changes in the topological structure of metal nanoparticles. Investigating the topological structure of LSPP-excited materials is of primary

importance for manipulating their optical properties. For instance, altering the size of metal nanoparticles, commonly achieved by changing the aspect ratio of metal nanorods, results in variations in the resonance frequency and intensity of SPPs [7]. Furthermore, modifying the morphological structure of the material also influences the coupling characteristics of SPPs [7]. Fig. 2 illustrates the optical properties of several classic SPPs materials with different morphologies [10]. For instance, spherical and square metal particles of 40nm in size exhibit optical attenuation peaks within the range of 300nm to 600nm. In the case of tetrahedrons, both the scattering and extinction coefficients tend towards zero, with a lower absorption coefficient, due to the tetrahedral geometrically symmetric structure [10]. Additionally, it has been observed that as the thickness of the nanofilm decreases, the optical attenuation peak of SPPs becomes sharper and exhibits a certain degree of redshift [10]. By employing various morphological structures, the optical response of SPPs becomes diversified, offering broad prospects for research on SPPs in the infrared region.

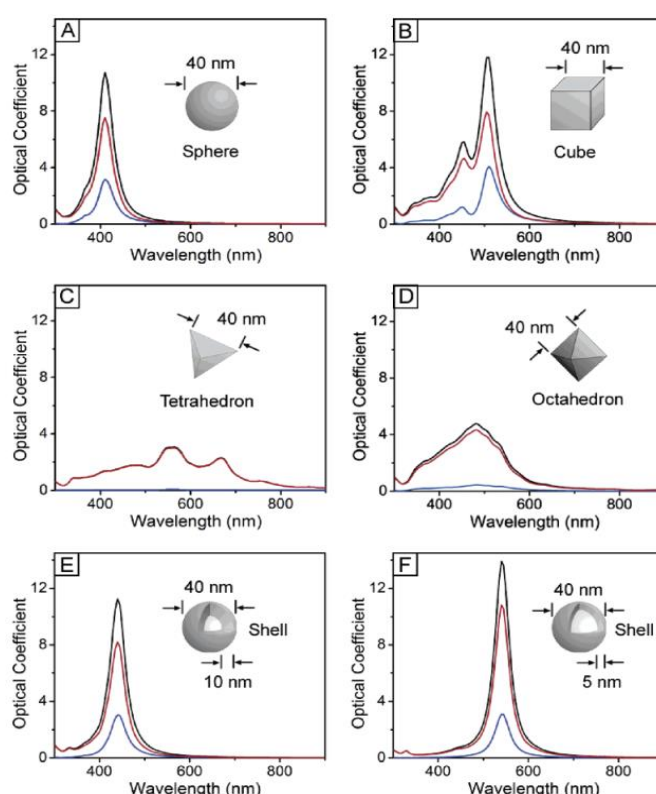


**Figure 2.** The extinction (black line), absorption (red line), and scattering (blue line) spectra of silver nanoparticles with different morphologies (extinction value=absorption value - scattering value): (a) Isotropic solid silver nanospheres; (b) Anisotropic solid silver cube; (c) Tetrahedron; (d) Octahedron; (e) Thick hollow silver particles; (f) Thin hollow silver particles

Currently, because of technological constraints, the difficulty of fabricating metal morphologies has increased, and researchers are no longer satisfied with simply altering the shape and structure of metal nanoparticles [8, 9]. As a result, the focus of research has shifted towards the study of dual-metal nanoparticle systems (or even multi-metal nanoparticle systems) that involve interactions between nanoparticles [11]. For single-gold nanoparticle systems, the background refractive index is the primary influencing factor for the resonance coupling frequency of SPPs [11]. For a dual-gold nanoparticle system, the most intuitive variable is the gap distance ( $w$ ) between the nanoparticles. The variation of gap distance affects the coupling strength between the nanoparticles and determines the extinction coefficient and resonant wavelength response [11]. The simulated optical responses of gold nanoparticle pairs under different gap distances using the FDTD algorithm are shown in Fig. 3 [11]. It can be observed that regardless of the change in nanoparticle gap distance, an optical redshift phenomenon occurs in the plasmon resonances with an increase in background refractive index. However, within the range of background refractive index  $n=1$  to  $n=1.3$  for each case, the amount of

redshift is different. It mainly exhibits a characteristic of first increasing and then decreasing, with the largest redshift observed for the case of  $w=5$  [11]. Nevertheless, under the same background refractive index  $n$ , the plasmon resonances exhibit a phenomenon of first red shifting and then blue shifting as the gap distance between the gold nanoparticles gradually increases [11]. This result is expected since the increased gap distance between the nanoparticles leads to a decrease in the number of mutual "hotspots" and a reduction in the coupling efficiency. It can be predicted that under the same background refractive index, there will be a maximum redshift wavelength for the gold nanoparticle system, which will limit the development of far-infrared SPPs technologies. Although the dual-sphere nanoparticle system provides a convenient means to modulate the optical response of SPPs, further research on different morphological structures and novel excitation methods for SPPs materials is still required, as the background refractive index cannot increase indefinitely.

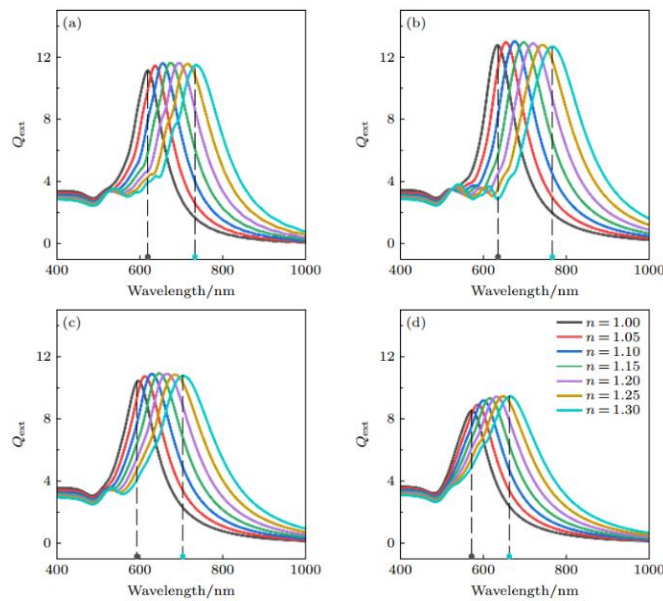


**Figure 3.** Extinction Spectra of Double Nanospheres with Different Spacing in Different Background Refractive Index( $n$ ): (a)  $w=2\text{nm}$ ; (b)  $w=5\text{nm}$ ; (c)  $w=10\text{nm}$ ; (d)  $w=20\text{nm}$

## 4. Generation of Surface Plasmon Polaritons

### 4.1. Common Coupling Excitation of Surface Plasmon Polaritons

From equation of SPPs dispersion, it can be seen that the wavevector of SPPs is always greater than the wavevector of incident light in vacuum, requiring special excitation methods. So far, the common methods for exciting SPPs are prism-coupled excitation and grating-coupled excitation, and different near-field optical excitation methods have been studied for various application domains [1, 12].

The core principle of prism-coupled excitation is based on the attenuated total reflection (ATR) principle, which was invented by Otto and Kretschmann. Therefore, the excitation setups can be divided into O-structure (Fig. 4(a)) and K-structure (Fig. 4(b)) [13]. Their common principle is that an exponentially decaying evanescent wave can tunnel through a low-index material with a small real part of refractive index, allowing the optical field to reach the surface of a high-index material (the metal surface for exciting SPPs) on the other side, thereby inducing the excitation of SPPs [13]. For the medium-metal-prism SPPs excitation setup, the wavevector compensated by the prism is given by:

$$\Delta k = k_{spp} - k_0 = \frac{\omega}{c} \left( \sqrt{\epsilon_{prism}} \sin \theta_{sp} - 1 \right) \quad (7)$$

Where  $\theta_{sp}$  is the angle of incidence of light from the prism to the metal, and it must be greater than the total internal reflection critical condition at the prism-metal interface. In addition to compensating the wavevector using a prism, the diffractive effect of a grating can also provide momentum compensation similar to that of a prism [12]. As shown in Fig. 4(b), SPPs grating excitation structures can be achieved by etching periodic grating structures on the surface of the metal material [12]. The wavevector compensation of the metal grating for SPPs is given by:

$$\Delta k = \frac{\omega}{c} (\sin \theta - 1) \pm mG \quad (8)$$

Where  $G$  is the grating constant, depending on the phase period of the grating  $\Lambda$ , and  $m$  is the grating order, taking positive integers. It can be observed that the wavevector matching condition of the grating is already limited during its fabrication. Therefore, although grating-coupled excitation of SPPs has high efficiency, it also suffers from the drawbacks of complex etching techniques and poor tunability [12].

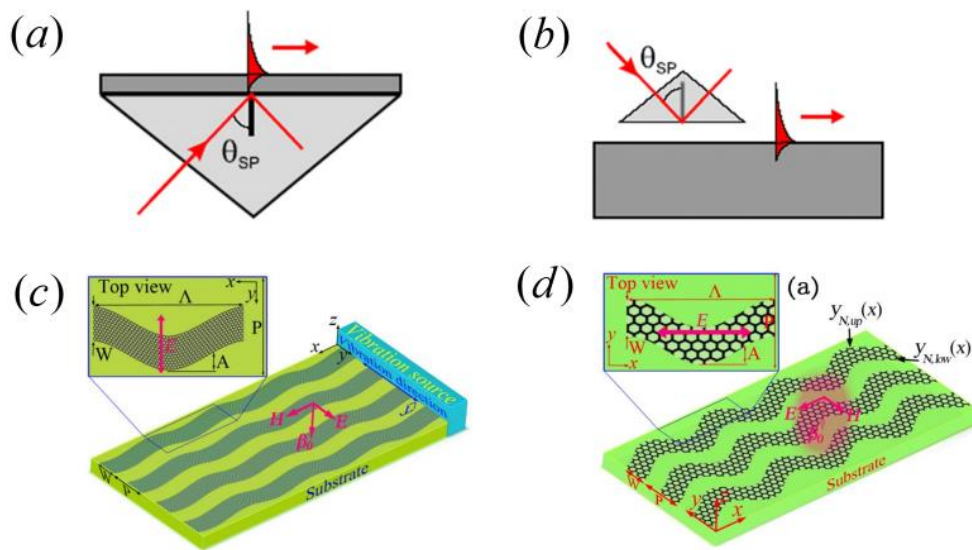


**Figure 4.** Excitation method of SPPs: (a) K-structure, (b) O-structure, (c) Longitudinal bending graphene grating structure, (d) Transverse bending graphene grating structure [1, 15]

#### 4.2. SPPs Excitation of Two Sinusoidal Graphene Grating Structures

Because of the strong morphological flexibility of two-dimensional materials such as graphene, the excitation mode of SPPs can be modified, providing more options for wavelength tuning [9, 14]. Based on the different bending directions of strip-shaped graphene, one can obtain transversely bent and longitudinally bent gratings. As shown in Fig. 4(c), due to the two-dimensional structure of graphene, one can extend infinitely in the  $x$ -direction and provide a continuously operating vibrational source in the  $z$ -direction, causing the graphene material to form a longitudinally inward-bent periodic grating with a period  $\Lambda$  [14]. The excitation approach of this material is similar to grating coupling, where the graphene material itself undergoes a grating-like morphological change, resulting in additional scattered wavevectors when the incident light is coupled in order to achieve the wavevector matching condition. Due to the unique two-dimensional morphological structures of graphene, the resulting SPPs modes will be significantly different [15]. The theoretically derived SP resonance modes of this structure based on the confined electron model of graphene can be expressed as:

$$\omega_p = \frac{e}{h} \sqrt{E_F / \pi \eta \epsilon_{avg} (W \pm 2A)} \quad (9)$$

Where  $E_F$  represents the Fermi energy level and  $h$  is Planck's constant.  $\epsilon_{avg}$  is the arithmetic mean of the dielectric constants on both sides of the graphene strip, and  $\eta$  is a parameter uniquely associated with the electromagnetic response [14, 15]. One can observe that under a given excitation environment, graphene possesses two distinct SP resonance modes, characterized by the two possible

directions of amplitude oscillation coefficients ( $W_{\pm A}$ ). This indicates the generation of two different SPPs modes within a graphene strip. Theoretical simulations have also suggested the existence of two new SPPs modes, referred to as "peak mode" and "valley mode," at the crest and trough positions of a sinusoidal grating graphene structure [14]. The underlying reasons for the emergence of these modes still lack theoretical derivation and experimental validation. However, it can be anticipated that due to the confinement effects of graphene nanostructures, the SPPs excited at the crest and trough exhibit distinct geometric boundary conditions, resulting in significantly enhanced localization properties of SPPs energy. The structural model of using mechanical vibrations to form a grating is complex and not conducive to integration in the field [14]. As shown in Fig. 4(d), another type of grating-coupled excitation structure can be achieved by transversely bending the graphene material into a strip, with the grating period remaining the same [14]. Because of the absence of continuous vibrating sources, the transversely bent graphene grating structure can be treated as a quasi-static case compared to the longitudinally bent structure [14]. By solving the expression of the SP resonance mode through the wavevector matching condition equation:

$$\omega_p = \sqrt{\frac{e^2 E_f M}{\hbar^2 \epsilon_0 \epsilon_{avg} \Lambda}} \quad (10)$$

Where  $M$ ,  $\Lambda$  represent the mode order of the incident light field and the actual period of the planar grating, respectively [14]. Unlike the longitudinally bent graphene grating structure, the transversely bent structure only generates a single SPPs optical mode [14]. Moreover, there is evidence indicating that in such a grating structure, the polarized SPs energy is mainly concentrated at the boundary positions of the nanoribbon, rather than the peak positions of a sinusoidal model [14].

It is worth noting that in both sinusoidal graphene structures, the Fermi level can be modulated by an external power source due to the high doping EHP concentration of graphene, enabling the control and modulation of SPPs excitation modes, which is not possible in non-two-dimensional materials [14]. Furthermore, the transversely bent structure exhibits a significantly high transmission spectrum quality factor  $Q$ , indicating the potential for ultra-narrowband filtering capabilities [14]. Additionally, the excitation structures composed of graphene wrapped on semiconductor oxides in an array configuration or the application of an external magnetic field to induce directional excitation effects have demonstrated the infinite possibilities of graphene in the field of SPPs [14, 15]. The grating graphene structure, as a sinusoidal structure, gives rise to the generation of various SPPs optical modes in optics. This implies that two-dimensional materials, based on their morphological plasticity, hold broad prospects in the fields of optics and even physics. However, most innovative materials still remain in the theoretical simulation stage, lacking experimental data support, let alone practical applications. Future research directions in SPPs should focus more on exploring practical feasibility.

## 5. Application of Surface Plasmon Polaritons

In history, unique phenomena of SPPs were discovered through metal accidents, and based on their irreplaceable light field localization and extremely strong energy density, SPPs have shown potential application prospects in various optical fields. According to the classification mentioned earlier, SPPs can be divided into propagation type and local type. According to different modulation mechanisms, propagating SPP modulators can be divided into several categories: all optical modulation, thermal modulation, electrical modulation, and magnetic modulation [16]. Introducing a VOA (Variable Optical Attenuator) modulator that utilizes epoxy resin as the cladding material and Ag as the SPP excitation material. The structure is depicted in Fig. 5(a), with dimensions of length, width, and height are  $10000 \times 10 \times 0.15 \mu m$ . The refractive index of the polymer cladding is 1.45, and an aluminum substrate is included to enable temperature manipulation [17]. This thermal modulator operates based on the principle of thermo-optic effects. The main modulation process involves heat transfer through the aluminum substrate, resulting in a temperature gradient within the epoxy resin cladding. The sensitivity of the material to temperature induces changes in the optical

refractive index. Fig. 5(b) illustrates the variation of temperature with device depth [17]. It is important to note that the thermo-optic coefficient (TOC) of the epoxy resin is negative, indicating that the refractive index of the upper cladding layer decreases with temperature compared to the lower layer [17]. SPPs are excited within the silver core, and the transition from symmetric SPP excitation to antisymmetric SPP excitation occurs, leading to increased losses and transmission suppression [1, 17]. This device cleverly exploits the specific transition from symmetric to antisymmetric structures, forming an optical switch characteristic. As shown in Fig. 5(c), when the applied voltage exceeds 2.5V, the optical signal in the waveguide experiences significant attenuation, resulting in suppression [17]. Additionally, Fig. 5(d) indicates that the transmission signal after 2.51V exhibits increased attenuation, indicating stronger signal noise and stable over a large spectral range [18].

This structure exhibits an extremely high extinction ratio (ER=28dB), demonstrating its enormous market potential. However, the system also suffers from excessive insertion loss due to factors such as thermal diffusion in the cladding material, making it impractical for actual production [17, 18]. Graphene, on the other hand, as a high-transmittance material, maintains low transmission losses and achievable low insertion loss while operating in the infrared absorption range.

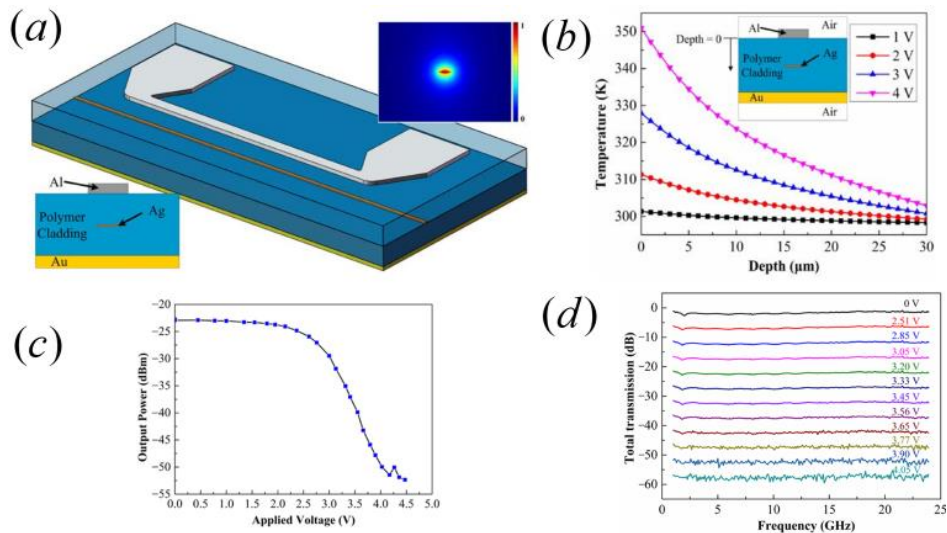


**Figure 5.** Structure diagram and parameter curve of variable optical attenuator (VOA): (a) structure and light field distribution of VOA, (b) the variation of device with depth under different voltages, (c) function curve of applied voltage and output power of VOA, (d) response characteristics of device response circuits under different applied voltages

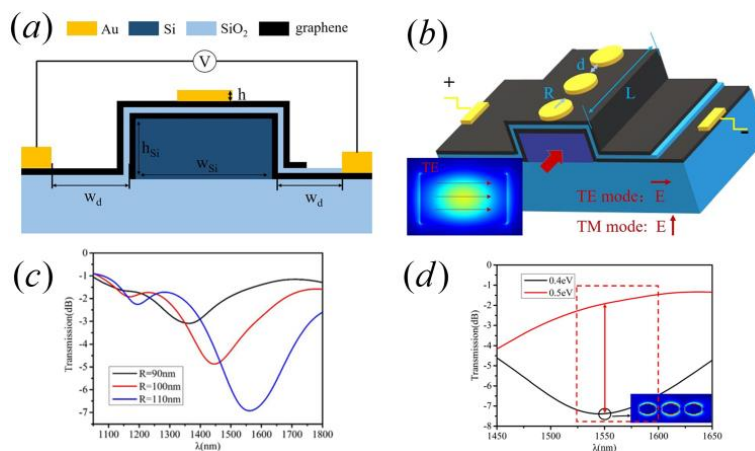


**Figure 6.** Structure and parameter curve of a SPP enhanced GOS modulator: (a) the cross-section of the modulator, (b) the 3D view and light field distribution, (c) the transmission spectrum of the modulator varies with the radius of the disk at parameters  $d=70\text{nm}$  and  $h=30\text{nm}$ , (d) Transmission spectrum of the device

For LSP modulators, most of the research focuses on thin two-dimensional materials such as graphene [18]. By fabricating SPP-graphene hybrid waveguides, the coupling efficiency of light can be enhanced and the device size can be reduced, overcoming the limitations of weak interaction between materials like graphene and light due to their small two-dimensional quantum space [17, 18]. As mentioned earlier, by changing the background refractive index, the coupling wavelength of SPPs can be red-shifted or blue-shifted, resulting in a mismatch between the material and the incident light frequency and producing an extinction effect. Therefore, LSP modulators typically utilize this principle to modulate signals in transmission circuits [18]. For example, Fig. 6(a) and Fig. 6(b) illustrate an LSP modulator fabricated based on the carrier modulation characteristics of graphene [19]. In this structure, a metal disk is placed on the graphene to excite the SPP mode, forming an SPP-graphene hybrid waveguide. The coupling strength of the device is adjusted by tuning the parameters of the metal disk, such as the diameter ( $d$ ), radius ( $R$ ), and height ( $h$ ), providing good adaptability [18]. Fig. 6(c) shows the simulated transmission spectrum obtained by varying the radius ( $R$ ) of the metal disk [18]. It can be observed that a larger metal disk leads to a stronger red-shift effect. However, if the metal disk is set too large, it will increase the device's footprint [18]. Fig. 6(d) presents the optimized transmission spectrum obtained by optimizing the parameters, with a driving voltage of 0.4 eV indicating the OFF state of the device [18].

Currently, there are numerous emerging nanoscale modulators based on novel technologies in addition to some typical traditional modulators. To compare the advantages and disadvantages of SPP modulators. As a matter of fact, SPP modulators have achieved performance standards comparable to traditional modulators in various aspects. Regarding extinction ratio, propagating SPP modulators can reach a high numerical value of 20dB. Due to the fact that most SPP modulators are based on graphene-coupled hybrid waveguide structures and inherit the low-loss characteristics of graphene, they possess great application potential in integrated optics and infrared communication fields in terms of energy consumption and insertion loss [16-20]. However, research on SPP modulators is still at an early stage. The relevant research literature and the systematic classification of optical modulators in the SPP field have not yet been well-established. This paper horizontally compares a few selected literature sources, aiming to lay a theoretical groundwork for future systematic studies in the SPP field.

Currently, many studies have emerged regarding metal-based SPP filters. However, because of significant propagation losses and limited tunability, metal-based SPP devices have certain drawbacks. To address these issues, Cai et al. proposed a concept for a highly tunable far-infrared filter device based on graphene [21]. This device consists of a structure composed of a graphene waveguide and two graphene-ribbon resonators with different lengths, allowing for the excitation of two distinct graphene surface plasmon (GSP) modes – edge mode and waveguide mode. These two modes exhibit independently tunable stopbands [21]. The research demonstrates that by adjusting the lengths of the graphene-ribbon resonators and the spacing between them and the graphene waveguide, the resonant frequency can be tuned between 13.3THz and 18.2THz. Moreover, the center frequencies of the two stopbands can be independently tuned by varying the applied voltage [21].

## 6. Limitation and Prospects

Surface Plasmon Polaritons are characterized by their unique localized optical field and potential to overcome the diffraction limit, making them crucial in the field of optics. However, research on various aspects of SPPs is still in its early stages, and truly gaining widespread attention requires more theoretical guidance and a deeper understanding of new phenomena. Currently, research in the field of SPPs is limited by several factors:

- High transmission losses: Due to the large imaginary part of the dielectric constant, SPPs struggle to achieve long-distance energy propagation, posing significant obstacles for waveguide applications and short-wave infrared signaling.

- Challenges and high costs in nanofabrication: Precise nanofabrication techniques, such as etching, are still imperfect, resulting in scarce experimental data, and commercialization of SPPs still has a long way to go.
- Demands for strong coupling and higher power density: Despite SPPs having extremely small dimensions and high energy density, achieving efficient coupling and device compatibility remains challenging. On one hand, new coupling technologies are yet to be realized; on the other hand, efficient integration schemes require further exploration.

Currently, scientific research in infrared spectroscopy is also encountering limitations in terms of scale and signal intensity. At the nanoscale, traditional optical techniques struggle to achieve sufficient spatial resolution, limiting in-depth investigations into microscopic physical processes. Additionally, due to the lower signal intensity compared to visible light, more sensitive techniques and equipment are required for detection and analysis of infrared spectra. Nevertheless, researchers have made significant progress in addressing these limitations. The combination of SPPs with graphene, for example, has yielded various noteworthy outcomes. Low-loss LR-SPP waveguides over longer distances have been achieved through graphene's low-loss carrier transmission. Furthermore, the strong tunability of graphene enables dynamic control of SPP devices, making infrared-responsive spectroscopy possible. By exploring the applications of SPPs in infrared spectroscopy, one can overcome current technological limitations and achieve a deeper understanding of microscopic physical and chemical processes. It is believed that more researchers will engage in these fields, resulting in further advancements and value creation.

## 7. Conclusion

Based on the content and structural sequence of the article, this study provides a clear introduction to surface plasmon polaritons by explaining the Maxwell's electromagnetic wave equations. It emphasizes the redshift characteristics of SPPs and the challenges of wavevector matching during excitation. The article systematically compares and categorizes SPP modulators, highlighting the redshift properties and adaptability of SPP resonances, demonstrating the versatility of SPP devices. Furthermore, it introduces SPP infrared filters and addresses the current technological limitations and immense future potential of SPPs. However, it is important to note that despite advancements, the study of SPPs is still in its early stages, and faces challenges such as incomplete theoretical frameworks and limited availability of research data. Nevertheless, with ongoing progress in fields like materials science and nanofabrication, research on SPPs is expected to grow, leading to the maturation of integrated optical technologies. Based on the comprehensive analysis of SPPs in the infrared domain, this article provides theoretical insights that could contribute to the resolution of challenges associated with far-infrared and even microwave optical devices.

## References

- [1] Zhang J, Zhang L, Xu W. Surface plasmon polaritons: physics and applications. *Journal of Physics D: Applied Physics*, 2012, 45 (11): 113001.
- [2] Wood R W. XLII. On a remarkable case of uneven distribution of light in a diffraction grating spectrum. *The London, Edinburgh, and Dublin Philosophical Magazine and Journal of Science*, 1902, 4 (21): 396-402.
- [3] Maystre D. Survey of surface plasmon polariton history. *Plasmonics: From Basics to Advanced Topics*. Berlin, Heidelberg: Springer Berlin Heidelberg, 2012: 3-37.
- [4] Cunningham S L, Maradudin A A, Wallis R F. Effect of a charge layer on the surface-plasmon-polariton dispersion curve. *Physical Review B*, 1974, 10 (8): 3342.
- [5] Chen Y, Tong C, Qin L, et al. Progress in surface plasmon polariton nano-laser technologies and applications. *Chin. Opt*, 2012, 5 (5): 453-463.

- [6] Zayats A V, Smolyaninov II, Maradudin A A. Nano-optics of surface plasmon polaritons. *Physics reports*, 2005, 408 (3-4): 131-314.
- [7] Yu H, Peng Y, Yang Y, et al. Plasmon-enhanced light-matter interactions and applications. *npj Computational Materials*, 2019, 5 (1): 45.
- [8] Lei S, Qi-Feng R, Jian-Fang W, et al. Localized surface plasmons. *Physics*, 2014, 43 (05): 290-298.
- [9] Cui Lin. *Research on Nonlinear Effects and Applications of Van der Waals Semiconductor and Surface plasmons*. Beijing University of Science and Technology, 2023.
- [10] Wiley B J, Im S H, Li Z Y, et al. Maneuvering the surface plasmon resonance of silver nanostructures through shape-controlled synthesis. *The Journal of Physical Chemistry B*, 2006, 110 (32): 15666-15675.
- [11] Wen X, Jian C, Li L, et al. Correlation of optical sensing with extinction coefficient and local field enhancement in gold nanosphere dimer. *ACTA PHYSICA SINICA*, 2021, 70 (9).
- [12] Dou X, Min C, Zhang Y, Yuan X. *Surface Plasmon Polaritons Optical Tweezers Technology*. *Acta Optica Sinica*, 2016, 36 (10): 1026004.
- [13] Welford K. Surface plasmon-polaritons and their uses. *Optical and Quantum Electronics*, 1991, 23: 1-27.
- [14] Xia Sn. *Excitation and Regulation of Plasmons on Graphene Surface*. Hunan University, 2018.
- [15] Gao W, Shu J, Qiu C, et al. Excitation of plasmonic waves in graphene by guided-mode resonances. *ACS nano*, 2012, 6 (9): 7806-7813.
- [16] Wen Z, Long G, Hong W, et al. Modulation of propagating surface plasmons. *Acta Physics Sinica*, 2019, 68 (14).
- [17] Tang J, Liu Y R, Zhang L J, et al. Flexible thermo-optic variable attenuator based on long-range surface plasmon-polariton waveguides. *Micromachines*, 2018, 9 (8): 369.
- [18] Luan J, Zheng P, Yang H, et al. A compact graphene modulator based on localized surface plasmon resonance with a chain of metal disks. *Plasmonics*, 2019, 14: 1949-1954.
- [19] Hu X, Feng S, Feng L, et al. Research Progress of Silicon-Based Photonic Modulator. *Journal of Integration Technology*, 2022, 11 (2):89-106.
- [20] Liu H, Guo H, Tan M, Li Z. Research progress of lithium niobate thin-film modulators. *Chinese Optics*, 2022, 15 (1): 1-13.
- [21] Cai Y, Da Xu K, Guo R, et al. Graphene-based plasmonic tunable dual-band bandstop filter in the far-infrared region. *IEEE Photonics Journal*, 2018, 10 (6): 1-9.